



Deposited via The University of Leeds.

White Rose Research Online URL for this paper:

<https://eprints.whiterose.ac.uk/id/eprint/112889/>

Version: Accepted Version

---

**Article:**

Zhai, X, Shi, J, Zou, X et al. (2017) Novel colorimetric films based on starch/polyvinyl alcohol incorporated with roselle anthocyanins for fish freshness monitoring. *Food Hydrocolloids*, 69. pp. 308-317. ISSN: 0268-005X

<https://doi.org/10.1016/j.foodhyd.2017.02.014>

---

© 2017 Elsevier Ltd. This manuscript version is made available under the CC-BY-NC-ND 4.0 license <http://creativecommons.org/licenses/by-nc-nd/4.0/>

**Reuse**

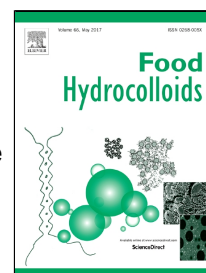
Items deposited in White Rose Research Online are protected by copyright, with all rights reserved unless indicated otherwise. They may be downloaded and/or printed for private study, or other acts as permitted by national copyright laws. The publisher or other rights holders may allow further reproduction and re-use of the full text version. This is indicated by the licence information on the White Rose Research Online record for the item.

**Takedown**

If you consider content in White Rose Research Online to be in breach of UK law, please notify us by emailing [eprints@whiterose.ac.uk](mailto:eprints@whiterose.ac.uk) including the URL of the record and the reason for the withdrawal request.

# Accepted Manuscript

Novel colorimetric films based on starch/polyvinyl alcohol incorporated with roselle anthocyanins for fish freshness monitoring



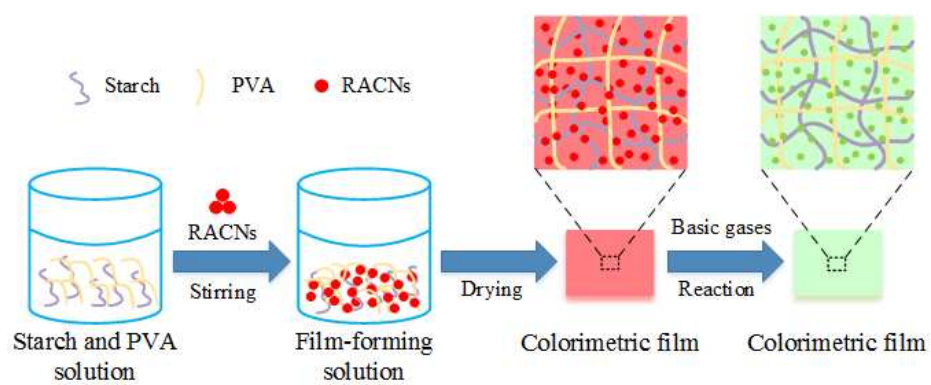
Xiaodong Zhai, Jiyong Shi, Xiaobo Zou, Sheng Wang, Caiping Jiang, junjun Zhang, Xiaowei Huang, Wen Zhang, Mel Holmes

PII: S0268-005X(16)30955-9  
DOI: 10.1016/j.foodhyd.2017.02.014  
Reference: FOOHYD 3804  
To appear in: *Food Hydrocolloids*  
Received Date: 05 December 2016  
Revised Date: 20 February 2017  
Accepted Date: 20 February 2017

Please cite this article as: Xiaodong Zhai, Jiyong Shi, Xiaobo Zou, Sheng Wang, Caiping Jiang, junjun Zhang, Xiaowei Huang, Wen Zhang, Mel Holmes, Novel colorimetric films based on starch /polyvinyl alcohol incorporated with roselle anthocyanins for fish freshness monitoring, *Food Hydrocolloids* (2017), doi: 10.1016/j.foodhyd.2017.02.014

This is a PDF file of an unedited manuscript that has been accepted for publication. As a service to our customers we are providing this early version of the manuscript. The manuscript will undergo copyediting, typesetting, and review of the resulting proof before it is published in its final form. Please note that during the production process errors may be discovered which could affect the content, and all legal disclaimers that apply to the journal pertain.

## Graphical abstract



**Highlights**

- Colorimetric films were developed by using roselle anthocyanins, starch and PVA.
- Roselle anthocyanins improved the [compatibility](#) between starch and PVA.
- The colorimetric films had good color stabilities within 14 days at 4°C and 25°C.
- The colorimetric film with fewer roselle anthocyanins was more sensitive to NH<sub>3</sub>.
- The colorimetric films can be used to monitor the fish freshness at 4°C.

1 **Novel colorimetric films based on starch/polyvinyl alcohol incorporated with**  
2 **roselle anthocyanins for fish freshness monitoring**

3

4 Xiaodong Zhai<sup>#1</sup>, Jiyong Shi<sup>#1</sup>, Xiaobo Zou<sup>##1</sup>, Sheng Wang<sup>1</sup>, Caiping Jiang<sup>1</sup>, junjun Zhang<sup>1</sup>,  
5 Xiaowei Huang<sup>1</sup>, Wen Zhang<sup>1</sup>, Mel Holmes<sup>2</sup>

6 <sup>1</sup> Agricultural Product Processing and Storage Lab, School of Food and Biological  
7 Engineering, Jiangsu University, Zhenjiang, Jiangsu 212013, China

8 <sup>2</sup> School of Food Science and Nutrition, the University of Leeds, Leeds LS2 9JT, United  
9 Kingdom

10 <sup>#</sup> These authors contributed equally to this study

11 <sup>\*</sup> Corresponding author. Tel.: +86 511 88780174; fax: +86 511 88780201. Email:  
12 [zou\\_xiaobo@ujs.edu.cn](mailto:zou_xiaobo@ujs.edu.cn)

14 **Abstract**

15 Novel colorimetric films were developed for real-time monitoring of fish freshness  
16 based on starch/polyvinyl alcohol (SPVA) incorporated with roselle (*Hibiscus*  
17 *sabdariffa* L.) anthocyanins (RACNs). Firstly, RACNs were extracted from roselle  
18 dehydrated calyxes. Secondly, SPVA aqueous solution was obtained with a mass rate  
19 of 2:1 (starch/PVA). Thirdly, the colorimetric films were fabricated by immobilizing  
20 30, 60 and 120 mg RACNs/100 g starch into SPVA matrix with casting/solvent  
21 evaporation method. FTIR spectra of the colorimetric films showed that RACNs were  
22 successfully immobilized into the SPVA matrix. X-ray diffraction spectra and SEM  
23 micrographs indicated that the crystallinity of PVA was reduced during the film-  
24 forming process and the compatibility between starch and PVA was improved, owing  
25 to the presence of RACNs. The incorporation of RACNs led to a decrease of water  
26 content and tensile strength and an increase of elongation at break of the colorimetric  
27 films compared with the SPVA film. The color stability test showed that the  
28 colorimetric films were stable at refrigeration temperature and room temperature up to  
29 14 days with relative color changes below than 5%. The colorimetric films with lower  
30 content of RACNs were found more sensitive towards ammonia. An application trial  
31 was conducted to monitor the freshness of silver carp (*Hypophthalmichthys molitrix*) at  
32 refrigeration temperature. The colorimetric films presented visible color changes over  
33 time due to a variety of basic volatile amines known as total volatile basic nitrogen  
34 (TVB-N). Hence, these colorimetric films can be used to monitor the real-time fish  
35 freshness for intelligent packaging.

36

37 **Keywords:** Colorimetric film; Fish freshness; Roselle anthocyanins; Starch; Polyvinyl  
38 alcohol; Intelligent packaging.

## 40 1. Introduction

41 Fish is highly perishable due to enzymatic reaction and microbial contamination  
42 (Zhang, Sun, Xiao, Liu, & Zheng, 2016). Considering the food quality and safety, it is  
43 essential to evaluate the fish freshness during the supply chain. TVB-N has been widely  
44 regarded as an useful indicator of the fish freshness for a long period (Olafsdóttir, et al.,  
45 1997). It is comprised of ammonia (NH<sub>3</sub>), trimethylamine (TMA) and dimethylamine  
46 (DMA) generated by the enzymatic decomposition of trimethylamine oxide (TMAO)  
47 (Byrne, Lau, & Diamond, 2002). A variety of approaches have been developed to  
48 determine the TVB-N level. Chemical methods such as Kjeldahl method can provide  
49 precise results, but they are generally time consuming and destructive to samples. Other  
50 rapid and non-destructive detection methods, such as FTIR spectroscopy, can also  
51 provide satisfactory results (Cai, Chen, Wan, & Zhao, 2011), whereas they need  
52 advanced instruments and highly skilled operators. Consequently, these methods are  
53 not suitable for consumers to evaluate the real-time freshness.

54 In the last decades, there was a rapidly growing interest in developing intelligent  
55 packaging systems for 'on-package' tracing the real-time food quality. Particularly,  
56 colorimetric indicators have received wide attentions because they can exhibit  
57 straightforward information by visible color changes. As regard to evaluating the fish  
58 freshness, Pacquit, et al. (2007) developed a colorimetric indicator by spin-coating  
59 bromocresol green onto a PET substrate. The color of the indicator gradually changed  
60 from yellow to green in response to the increasing TVB-N level at room temperature.  
61 Similarly, polyaniline-based colorimetric indicator has also been demonstrated to detect  
62 the fish spoilage (Kuswandi, et al., 2012). These colorimetric indicators fixed in the  
63 headspace of the packaged fish presented specific color changes upon reaction with the  
64 TVB-N in the form of gas sensors. In this way, these intelligent packaging systems had  
65 great potential to indicate the real-time fish freshness.

66 Recently, more researches have focused on the natural pigments as a source of  
67 color agents, because they are safer and more eco-friendly as compared to  
68 chemosynthetic dyes. Anthocyanins are natural water-soluble pigments that have wide

69 response ranges to pH variation. Several kinds of anthocyanins have been utilized to  
70 fabricate the colorimetric indicators for sensing the food quality, such as anthocyanins  
71 extracted from red cabbage (Pereira, de Arruda, & Stefani, 2015), grape skin (Ma &  
72 Wang, 2016) and purple sweet potato (Choi, Lee, Lacroix, & Han, 2017). Zhang, Lu,  
73 and Chen (2014) developed a pH sensing film by incorporating anthocyanins extracted  
74 from *Bauhinia blakeana* Dunn with chitosan and the pH sensing film presented a  
75 distinguishable color change from purple to green due to the basic volatile gases  
76 generated from the fish, suggesting that the anthocyanins-based colorimetric films were  
77 good candidates of gas sensors for monitoring fish freshness. When a constant amount  
78 of fish samples was stored in a specific circumstance (e.g. temperature, packaging  
79 volume), the concentration of the TVB-N in the headspace was definite after a specific  
80 period of storage. Therefore, the extent of color change of the colorimetric film was  
81 related to the content of the anthocyanins. However, the effect of the anthocyanins  
82 content on color rendering properties of the colorimetric film has not been investigated  
83 yet.

84 Roselle (*Hibiscus sabdariffa* L.) is an herbaceous plant, cultivated largely in  
85 tropical and subtropical areas of both hemispheres (Sinela, et al., 2017). Its calyxes  
86 contain high amounts of anthocyanins up to 1.5 g/100 g on dry weight basis  
87 (Degenhardt, Knapp, & Winterhalter, 2000). The biological activities of roselle  
88 anthocyanin (RACNs), such as antioxidant activity (Tsai, McIntosh, Pearce, Camden,  
89 & Jordan, 2002) and anti-hypertensive effect (Ajay, Chai, Mustafa, Gilani, & Mustafa,  
90 2007) have been widely studied, while the potential use of RACNs for the development  
91 of colorimetric indicators has not been explored. In order to immobilize the  
92 anthocyanins, several natural polymers have been used for making different  
93 colorimetric films, including chitosan (Zhang, et al., 2014), starch (Choi, et al., 2017;  
94 Golasz, Silva, & Silva, 2013) and cellulose (Ma, et al., 2016). Among them, starch has  
95 received greater attention because of its stability to heat, acid and base conditions.  
96 However, pure starch film generally lacks the strength and processability, which can be  
97 alternatively addressed by adding polyvinyl alcohol (PVA) (Sin, Rahman, Rahmat, &  
98 Mokhtar, 2011). Since 1980s, starch/polyvinyl alcohol (SPVA) films have been studied

99 for packaging applications (Tang, Zou, Xiong, & Tang, 2008; Tang & Alavi, 2011).  
100 They have good transparency (Cano, Cháfer, Chiralt, & González-Martínez, 2015),  
101 which is beneficial for the development of colorimetric films. Furthermore, starch and  
102 PVA are both non-toxic, renewable and biodegradable (Lu, Xiao, & Xu, 2009; Rezaei,  
103 Nasirpour, & Fathi, 2015), which can eliminate the public concerns over food safety  
104 and environmental problems.

105 Therefore, in this study, we aimed to develop new colorimetric films by  
106 incorporating various content of RACNs into SPVA matrix through casting/solvent  
107 evaporation method. The microstructure of colorimetric films was studied by using X-  
108 ray diffractometer and SEM. The effect of the RACNs content on mechanical  
109 properties, color stability and sensitivity toward ammonia of the colorimetric films was  
110 investigated. Finally, the colorimetric films were employed to monitor the freshness of  
111 silver carp (*Hypophthalmichthys molitrix*) at refrigeration temperature (4°C).

## 112 2. Material and methods

### 113 2.1. Materials

114 Roselle dehydrated calyces and live silver carp were obtained from the local market  
115 in Zhenjiang, China. Other materials including soluble starch, polyvinyl alcohol (MW:  
116  $1750 \pm 50$ ), ethyl alcohol ( $C_2H_6O$ ), potassium chloride (KCl), sodium acetate  
117 ( $CH_3COONa \cdot 3H_2O$ ), magnesium oxide (MgO), methyl red ( $C_{15}H_{15}N_3O_2$ ), methylene  
118 blue ( $C_{16}H_{18}ClN_3S$ ), boric acid ( $H_3BO_3$ ), ammonia solution ( $NH_3 \cdot H_2O$ , 25%~27%),  
119 acetic acid ( $CH_3COOH$ ) and hydrochloric acid (HCl) were all purchased from  
120 Sinopharm Chemical Reagent Co., Ltd (Shanghai, China). Plastic Petri dishes were  
121 purchased from Sigma Chemical Co. (St. Louis, MO, USA).

### 122 2.2. Extraction of anthocyanins from roselle dehydrated calyces

123 The anthocyanins were extracted according to Chang, et al. (2012) with a slight  
124 modification. The roselle dehydrated calyces were crushed and blended with 75%  
125 ethanol aqueous solution at a solid–liquid ratio of 1:10 for 2 h at 25°C. The extract was  
126 centrifuged at 8000 rpm for 20 min. The extraction procedure was repeated three times.

127 Ethanol in filtrate was removed with a rotary evaporator at 35°C in dark. Finally, the  
128 solution was freeze-dried under vacuum and the obtained anthocyanins extract powder  
129 was stored in sample vials at 4°C in the nitrogen atmosphere.

### 130 2.3. Determination of total anthocyanins content in extract powder

131 The anthocyanins content in extract powder was measured by pH differential  
132 method (Wang, Li, Chen, Xin, & Yuan, 2013) using a UV-Vis spectrophotometry  
133 (Agilent CARY 100, Varian Corporation, USA). The anthocyanins extract powder (20  
134 mg) was dissolved in 10 mL distilled water, and 1 mL anthocyanins solution was  
135 dissolved in 9 mL of 0.025 M potassium chloride buffer (pH 1.0) and 9 mL of 0.4 M  
136 sodium acetate buffer (pH 4.5) respectively in separate test tubes. Absorbance of  
137 sample was measured at 520 and 700 nm. The anthocyanins content was expressed in  
138 mg/g.

### 139 2.4. Preparation of the colorimetric films

140 Firstly, 100 mL aqueous dispersion containing 2 g starch and 1 g PVA was heated  
141 at 100°C in a water bath and stirred with a magnetic stirrer until it was completely  
142 dissolved. Based on the calculated anthocyanins content ( $9.51 \pm 0.41$  mg/g) (refer to  
143 section 2.3), a certain amount of anthocyanins extract powder was then added to the  
144 cooled SPVA solution at 30, 60 and 120 mg RACNs/100 g starch, expressed as  
145 RACNs-30, RACNs-60 and RACNs-120, respectively. The mixtures were then  
146 homogenized (Ultra Turrax IKA T25 digital, Germany) at 8000 rpm for 5 min and  
147 degassed with a sonicator (Branson CPX5800H, USA) for 5 min at room temperature.  
148 Each film was prepared by casting 10 mL of the film-forming solution into a clean and  
149 smooth plastic Petri dish with a 53 mm diameter. The Petri dishes were placed on a  
150 level surface in an incubator at 35°C with 50% RH for 36 h. After that, the films were  
151 peeled from the Petri dishes and stored at 4°C with 75% RH for further use.

### 152 2.5. Spectral characteristic of RACNs

153 The color and spectra of RACNs solution at different pH (2-12) were recorded  
154 using a UV-Vis Spectrophotometer (Agilent CARY 100, Varian Corporation, USA) in

155 the range of 400-800 nm.

## 156 2.6. Characterization of the colorimetric films

### 157 2.6.1. FTIR spectroscopy

158 Fourier transform infrared (FTIR) spectra of the films were determined with a  
159 FTIR spectrometer (Perkine Elmer 16 PC spectrometer, Boston, USA). Spectra were  
160 recorded at the absorbance mode from 4000 to 650  $\text{cm}^{-1}$  at a resolution of 4  $\text{cm}^{-1}$  and  
161 the total number of scans was 32. OMNIC Spectra software (Thermo Scientific Co.,  
162 USA) was used to configure the FTIR spectrometer for scanning and mathematical  
163 processing.

### 164 2.6.2. X-ray diffraction spectra

165 X-ray diffraction (XRD) spectra of films were measured using an X-ray  
166 diffractometer (D8 ADVANCE, Bruker, Germany) with a reference of target of Cu Ka  
167 radiation, voltage of 40 kV, current of 30 mA. The films were measured at an angle  
168 from 5° to 40° ( $2\theta$ ) with steps of 2° ( $2\theta$ )/min.

### 169 2.6.3. Scanning electron microscopy (SEM)

170 The micrographs of the films were recorded by a field emission scanning electron  
171 microscopy (FE-SEM) (S-4800, Hitachi High-Technologies corporation, Japan). The  
172 films were first freeze-fractured by liquid nitrogen before measurement. Samples were  
173 attached to double-sided adhesive tape and mounted on the specimen holder, then  
174 sputtered and coated with gold under vacuum.

### 175 2.6.4. Thickness, water content and mechanical properties of the films

176 The thickness of the films was measured by a hand-held digital micrometer  
177 (Sanfeng Group Co., Ltd., Taiwan, China). The thickness was measured at 20 random  
178 positions on the films.

179 To determine the moisture content (MC), the films were dried to an equilibrium  
180 weight at 105°C in an oven. MC was calculated according to the following equation:

$$181 \quad MC(\%) = 100 \times (M_i - M_f) / M_i \quad (1)$$

182 where  $M_i$  was the initial weight of films stored in 75% RH to moisture equilibrium (g)  
 183 and  $M_f$  was the final weight of films dried at 105°C (g).

184 Tensile strength (TS) and elongation at break (EB) were measured with an Instron  
 185 Universal Testing Machine (Model 4500, Instron Corporation, Canton, MA, USA)  
 186 using a modified ASTM D882-00 (ASTM, 2000b) procedure. Each film was cut in  
 187 rectangular strips with 40 mm length and 20 mm width. The initial grip separation and  
 188 crosshead speed were set at 20 mm and 0.6 mm/s, respectively. Measurements represent  
 189 an average of three samples. The TS and EB were calculated as the following equations:

$$190 \quad TS = F_{\max} / S \quad (2)$$

$$191 \quad EB = 100 \times \Delta l / l_0 \quad (3)$$

192 where  $TS$  was the tensile strength (MPa);  $F_{\max}$  was the maximum load (N);  $S$  was the  
 193 initial cross-sectional area of the film sample (mm<sup>2</sup>);  $EB$  was the elongation at break;  
 194  $\Delta l$  was the extension of the films (mm) and  $l_0$  was the initial length of the films (20 mm).

#### 195 2.6.5. Color stability of the colorimetric films

196 The colorimetric films were stored in incubators at 4°C and 25°C with 75% RH  
 197 under fluorescent lights. The images of the colorimetric films were captured every day  
 198 for two weeks by an optical scanner (Scanjet G4050, HP) and analyzed by a user  
 199 program in Matlab R2012a (Matworks Inc., Natick, MA, USA). The stability of the  
 200 colorimetric films was defined as the relative color change (Xiaowei, et al., 2015):

$$201 \quad \Delta R = |R_0 - R_1| \quad (4)$$

$$202 \quad \Delta G = |G_0 - G_1| \quad (5)$$

$$203 \quad \Delta B = |B_0 - B_1| \quad (6)$$

$$204 \quad S = \frac{\Delta R + \Delta G + \Delta B}{R_0 + G_0 + B_0} \times 100\% \quad (7)$$

205 where  $R_0$ ,  $G_0$ ,  $B_0$  were the initial gray values of the red, green and blue,  $R_1$ ,  $G_1$ ,  $B_1$  were  
 206 the gray values of the red, green and blue after storage.  $S$  was the relative color change

207 of *R*, *G* and *B* values.

#### 208 2.6.6. Response of the colorimetric films to ammonia

209 Response of the colorimetric films toward volatile ammonia in term of their color  
210 changes was performed using absorbance measurements (Kuswandi, et al., 2012). The  
211 colorimetric films were cut into squares (10 × 10 mm) and hang up in an erlenmeyer  
212 flask (500 mL) at 1 cm above the ammonia solution (80 mL, 8 mM) for 24 min at 25°C.  
213 UV-vis spectra of the films in the range of 400-800 nm were recorded every 2 min by  
214 a hand-held fiber optical vis-NIR spectrometer (Ocean Optics Co., Ltd, USA).

#### 215 2.7. Application of the colorimetric films for monitoring fish freshness

##### 216 2.7.1. Fish spoilage trial

217 Live silver carp was cut into strips after removing its innards, head, tail and  
218 feathers. Then, 20 g of silver carp was immediately transferred into covered Petri dishes  
219 with 90 mm diameters. The colorimetric films were placed in the headspace of the Petri  
220 dish. The Petri dishes were stored in a refrigerator at 4°C for 165 h. The color of the  
221 colorimetric films was recorded after every 15 h by using the optical scanner.

##### 222 2.7.2. Determination of TVB-N

223 The TVB-N level of the fish sample was measured by a steam distillation method  
224 (Cai, et al., 2011). The 10 g portion was placed in a beaker, blended with 100 mL  
225 distilled water, then grounded by using a tissue homogenizer (A-88, Jintan medical  
226 instrument plant, China). The homogenate was filtered by using filter papers. Then, 5.0  
227 mL filtrate was transferred to Kjeldahl distillation unit (ZLQ03, East China Glass Co.  
228 Ltd., China) with addition of 5 mL 1% magnesium oxide suspension (1 g/L). The  
229 distillate was collected in a flask containing 10 mL 2% aqueous solution of boric acid  
230 and 3 droplets of mixed indicator produced from dissolution of 0.2 g of methyl red and  
231 0.1 g of methylene blue to 100 mL of ethanol. After that, the boric acid solution was  
232 titrated with a 0.01 M hydrochloric acid solution. TVB-N value was determined by the  
233 hydrochloric acid used during titration.

### 234 3. Results and discussion

#### 235 3.1. Color and spectral properties of RACNs

236 Fig. 1a shows the color change of RACNs solutions in the pH range of 2 to 12. It  
237 can be seen that the color of RACNs solutions was pink at pH lower than 5, and changed  
238 gradually to purple at pH 6-7. When the solutions were basic, the color altered to blue  
239 and yellow at pH 8-9 and 10-12, respectively. The UV-vis spectra of RACNs solutions  
240 corresponding with color changes were recorded, as shown in Fig. 1b. When the pH  
241 value was lower than 4, the maximum absorption peak was obtained at 520 nm and the  
242 absorbance gradually decreased with the increase of pH value. As the pH increased  
243 from 5 to 8, the maximum absorption peak showed a bathochromic shift from 540 to  
244 580 nm, accompanied with an increase of maximum absorbance. Furthermore, the  
245 absorbance at 580 nm decreased with the increase of pH in the range of 8-12.

246 The color variation and the corresponding peak shift was originated by their  
247 structure transformation (Castañeda-Ovando, Pacheco-Hernández, Páez-Hernández,  
248 Rodríguez, & Galán-Vidal, 2009). Different anthocyanins generally demonstrate  
249 different color response to pH variation (Garber, Odendaal, & Carlson, 2013). Herein,  
250 the color response of the crude RACNs extract solution was an integrated color  
251 response of several kind of anthocyanins, mainly including delphinidin-3-sambubioside  
252 and cyanidin-3-O-sambubioside (Grajeda-Iglesias, et al., 2016).

253 **Fig. 1**

#### 254 3.2. Characterization of the colorimetric films

##### 255 3.2.1. FTIR analysis

256 Fig. 2 shows FTIR spectra of the starch, PVA, RACNs, SPVA film and the  
257 colorimetric films. In the spectrum of starch, the broad band at 3289  $\text{cm}^{-1}$  and the peak  
258 at 1639  $\text{cm}^{-1}$  were attributed to the stretching vibration and bending vibration of O-H,  
259 respectively. The peak at 2924  $\text{cm}^{-1}$  corresponded to bending vibration of C-H. The  
260 characteristic peak occurred at 1639  $\text{cm}^{-1}$  was the feature of tightly bound water present  
261 in starch. The bands from 761 to 1077  $\text{cm}^{-1}$  corresponded to the C-O bond stretching

262 (Xu, Kim, Hanna, & Nag, 2005). The spectrum for PVA showed the maximum  
263 absorption peak at  $1086\text{ cm}^{-1}$  resulting from the C-O bond stretching and the peak at  
264  $1416\text{ cm}^{-1}$  corresponding to bending vibration of CH-CH<sub>2</sub> certified the basic carbon  
265 skeleton of PVA (Pereira, et al., 2015). In terms of RACNs spectrum, the peaks between  
266  $2800\text{-}3300\text{ cm}^{-1}$ , and the peaks at  $1709$  and  $923\text{ cm}^{-1}$  were the three characteristic bands  
267 for the recognition of carboxyl group, assigned to the stretching vibration of O-H and  
268 C=O, and the out-of-plane bending vibration of -OH, respectively. The peak at  $1596$   
269  $\text{cm}^{-1}$  was related to the combinations and overtones of aromatic compounds (Pereira, et  
270 al., 2015). The anthocyanins spectrum showed the maximum absorption peak at  $1023$   
271  $\text{cm}^{-1}$ , corresponding to aromatic ring C-H deformation. No significant difference  
272 between the spectra of colorimetric films could be observed. However, compared with  
273 the spectrum of SPVA film, a new peak around  $1627\text{ cm}^{-1}$  which was related to the  
274 combinations and overtones of aromatic compounds appeared in the spectra of the  
275 colorimetric films, certifying that RACNs have been incorporated into the starch/PVA  
276 matrix.

Fig. 2

277

### 278 3.2.2. XRD analysis

279 For starch granules, there are usually A, B, and C-type by XRD spectra because  
280 of their different crystalline structures (Buléon, Colonna, Planchot, & Ball, 1998; Tian,  
281 Rickard, & Blanshard, 1991). A-type starch has strong diffraction peaks at about  $15^\circ$   
282 and  $23^\circ$  and unresolved doublet at around  $17^\circ$  and  $18^\circ$ , while B-type starch possess the  
283 strongest diffraction peak at around  $17^\circ$ , some small peaks at around  $15^\circ$ ,  $20^\circ$ ,  $22^\circ$  and  
284  $24^\circ$ , and a characteristic peak at about  $5.6^\circ$  (Guo, Liu, Lian, Li, & Wu, 2014). C-type  
285 starch is a mixture of A and B-type starch. As shown in Fig. 3, the starch showed the  
286 strongest diffraction peaks at  $17.1^\circ$ , and weak peaks at  $15.1^\circ$ ,  $19.8^\circ$ ,  $22.2^\circ$  and  $24.1^\circ$ .  
287 The weakest characteristic peak at  $5.7^\circ$  was also observed. The results indicated that  
288 the starch granules were B-type. In the diffractogram of PVA, the peaks at around  $11.6^\circ$ ,  
289  $19.4^\circ$ ,  $23.0^\circ$  and the small hump at around  $40.8^\circ$  were associated to its crystalline  
290 structure (Sreekumar, Al-Harathi, & De, 2012).

291 As to the X-ray diffraction of SPVA film, no characteristic peak of starch granule  
292 appeared, which indicated that starch was well-dispersed in the SPVA film without  
293 crystalline structure, because the crystalline regions of starch granules were destroyed  
294 by heating and mechanical stirring during gelatinization. The broad peak in the range  
295 of 10-17° resulted from the amorphous state of starch in the SPVA film. However, there  
296 was a characteristic peak of PVA at 19.4°, indicating that there was partial crystal  
297 structure of PVA remained during the film-forming process. As regarded to the  
298 colorimetric films, the peak areas at 19.4° were smaller than that of SPVA film, and  
299 decreased with the increase of RACNs content. This indicated that there were fewer  
300 rearrangement of PVA molecules to crystallization. This phenomenon was probably  
301 due to the hydrogen bond formed between hydroxyl groups of anthocyanins and PVA.  
302 The dispersed phase of PVA molecules would be beneficial for the uniformity of films.

Fig. 3

303

### 304 3.2.3. SEM micrographs analysis

305 The cross-section of the SPVA film and colorimetric films are shown in Fig. 4. It  
306 could be observed that the SPVA film showed a two-phase structure. The continuous  
307 phase on the left was the starch-rich phase, while the network-like phase on the right  
308 was the PVA-rich phase. This structure was due to a certain degree of immiscibility  
309 between starch and PVA, which was also observed in a previous research (Cano,  
310 Cháfer, Chiralt, & González-Martínez, 2015). However, when RACNs were  
311 incorporated into the SPVA film, the cross-section of colorimetric films became  
312 homogeneous without phase separation. This implied that RACNs had excellent  
313 compatibility with SPVA, and simultaneously improved the compatibility between  
314 starch and PVA. Generally, the compatibility of starch and PVA can be improved by  
315 adding plasticizers such as glycerol, sorbitol, poly(ethylene glycol) and  
316 monosaccharides (Jiang, et al., 2012). These plasticizers contain a number of hydroxyl  
317 groups that can form intermolecular hydrogen bonds with the hydroxyl groups of starch  
318 and PVA and thus reduce the intermolecular hydrogen bonds and entanglements  
319 between polymer chains (Jiang, et al., 2012). In this work, the enhanced compatibility

320 between starch and PVA may also be ascribed to the hydrogen bonds between the  
321 hydroxyl groups of RACNs, starch and PVA. Furthermore, the cross-sections of the  
322 colorimetric films became more compact as a result of an increasing content of RACNs,  
323 indicating the more intensive interactions.

324 **Fig. 4**

#### 325 3.2.4. Thickness, water content and mechanical properties of the films

326 Table 1 shows the thickness, water content and the mechanical properties of the  
327 SPVA film and the colorimetric films. The SPVA/RACNs-120 film had the highest  
328 thickness, and no significant difference was observed between the thicknesses of the  
329 SPVA film, SPVA/RACNs-30 film and SPVA/RACNs-60 film. The water content  
330 (*WC*) of SPVA/RACNs-30 film was close to the SPVA film. However, when the  
331 RACNs content was higher than 60 mg/100 g starch, the *WC* of films significantly  
332 decreased with the increase of RACNs content. This was probably because the  
333 interaction between SPVA and RACNs could lower the availability of hydroxyl groups  
334 of SPVA, which would in turn limit the SPVA-water interactions (Wang, Dong, Men,  
335 Tong, & Zhou, 2013). The content of RACNs also had significant effect on the  
336 mechanical properties of the films. As can be seen, the tensile strength (*TS*) decreased  
337 with RACNs addition increasing from 30 to 120 mg/100 g starch, while the elongation  
338 at break (*EB*) increased with the increase of RACNs content. A similar behavior was  
339 found in SPVA films incorporated with hydroxyl group-riched glycerol (Yoon,  
340 Chough, & Park, 2006). The decrease of *TS* could be due to that the intramolecular  
341 interaction of starch molecules and PVA molecules was interrupted by the RACNs  
342 molecules, whereas the increase of *EB* was because the RACNs improved the  
343 compatibility of starch and PVA so that the films became more homogeneous, as shown  
344 in section 3.2.3, which resulted in enhanced extensibility.

345 **Table 1**

#### 346 3.2.5. Color stabilities of the colorimetric films

347 The self-stabilities of the colorimetric films were essential to their color

348 performance. Fig. 5 shows the relative color changes ( $S$ ) of the colorimetric films. It  
349 can be seen that the colorimetric films stored at 4°C had small  $S$  values which were  
350 lower than 1% within 14 days, showing that they had excellent color stabilities. There  
351 was no obvious difference between the  $S$  values of the colorimetric films with different  
352 content of RACNs. By contrast, the colorimetric films had higher  $S$  values when they  
353 were stored at 25°C. Obvious increase of  $S$  values can be observed in the first day, which  
354 may be due to the moisture equilibrium process of the colorimetric films with the  
355 surrounding environment. After that, the  $S$  values gradually increased with time, this  
356 was owing to that RACNs were partially oxidized by the oxygen. Furthermore, the  $S$   
357 values of the colorimetric films decreased with the increase of RACNs content,  
358 indicating that the colorimetric films with more RACNs possessed greater color  
359 stabilities. Nevertheless, the  $S$  values were overall lower than 5%, implying that the  
360 colorimetric films had great color stabilities at 25°C as well.

361 Generally, the isolated anthocyanins are highly unstable and their stabilities are  
362 affected by several factors such as pH, storage temperature, chemical structure, light,  
363 oxygen, and their concentration (Castañeda-Ovando, et al., 2009). The color stability  
364 of RACNs solution stored at different temperatures has been studied by Sinela, et al.  
365 (2017) who found that the RACNs solution had great stability at 4°C. Apart from the  
366 storage temperature, in this work, the great color stabilities of the colorimetric films  
367 may be, on one hand, owing to the low water content of the colorimetric films that  
368 reduced the hydration of anthocyanins thus preserving the color (Lewis, Walker, &  
369 Lancaster, 1995). On the other hand, starch and PVA may protect the anthocyanins  
370 from being oxidized to some extent by entrapping the anthocyanins. Moreover, the  
371 RACNs incorporated into the colorimetric films were crude extract, in which the co-  
372 pigments such as sugar and phenolic acids could contribute to the color stability of  
373 anthocyanins (Sui, Bary, & Zhou, 2016).

374 **Fig. 5**

### 375 3.2.6. Response of colorimetric films to ammonia vapor

376 In order to find out the response behavior of the colorimetric films towards the

377 volatile basic gas, the colorimetric films were exposed to the ammonia generated from  
 378 the 8 mM ammonia solution under 25°C for 24 min and UV-vis spectra were recorded.  
 379 The initial maximum absorption peak were all observed at 540 nm for these three  
 380 colorimetric films as shown in Fig. 6a, b and c, indicating a red shift compared with the  
 381 RACNs solution (520 nm). Similar red shift was also observed in chitosan films  
 382 containing bauhinia blakeana dunn anthocyanins (Zhang, et al., 2014). The absorption  
 383 peak at 540 nm decreased and another absorption peak at 640 nm gradually increased  
 384 with reaction time. These results indicated that the colorimetric films gradually  
 385 transferred to be more basic. The absorbance ratio at 640 nm versus 540 nm ( $A_{640}/A_{540}$ )  
 386 represented the green color intensity compared to the red color intensity (Choi, et al.,  
 387 2017), which increased with time as shown in Fig. 6d. The calibration curves showed  
 388 that  $A_{640}/A_{540}$  increased exponentially with the reaction time as the following formulas,  
 389 where x was the reaction time and y was  $A_{640}/A_{540}$ :

$$390 \quad y = 0.1235e^{0.0644x}, R^2 = 0.992, \text{ for SPVA/RACNs-30 film;} \quad (8)$$

$$391 \quad y = 0.0917e^{0.0611x}, R^2 = 0.9965, \text{ for SPVA/RACNs-60 film;} \quad (9)$$

$$392 \quad y = 0.0505e^{0.0059x}, R^2 = 0.9819, \text{ for SPVA/RACNs-120 film.} \quad (10)$$

393 The slope of calibration curve represented the rate of color variation from red to  
 394 green, a greater slope indicated a higher variation rate. At a certain reaction time, the  
 395 SPVA/RACNs-30 film had the highest color variation rate, followed by the  
 396 SPVA/RACNs-60 film and then the SPVA/RACNs-120 film. This result indicated that  
 397 the colorimetric film with fewer RACNs was more sensitive to  $\text{NH}_3$ . The color variation  
 398 mechanism of the colorimetric films was that the volatiled  $\text{NH}_3$  firstly combined with  
 399  $\text{H}_2\text{O}$  contained in the colorimetric film to form  $\text{NH}_3 \cdot \text{H}_2\text{O}$  which then hydrolyzed to  
 400 produce  $\text{NH}_4^+$  and  $\text{OH}^-$ , the latter of which induced the color change of RACNs. The  
 401 higher color variation rate occurred in the colorimetric films with fewer RACNs was  
 402 due to that the discolored RACNs took higher proportions of the total RACNs within  
 403 the same reaction time. It was generally expected that gas sensors could have fast  
 404 response to the analytes. Hence, the SPVA/RACNs-30 film that exhibited the highest  
 405 color variation rate would contribute to its application as a gas sensor.

Fig. 6

406

## 407 3.3. Trials on monitoring the fish freshness

408 TVB-N level was used as the indicator to determine the fish freshness. As shown  
409 in Fig. 7a, the initial TVB-N value of the fresh fish was 6.61 mg/100 g, and then it  
410 increased up to 28.53 mg/100 g at 165 h. According to Chinese Standard (GB 2733-  
411 2015), the rejection limit of TVB-N level for silver carp is 20 mg/100 g. This implied  
412 that the fish sample could not be consumed almost after 135 h.

413 The color changes of the colorimetric films were shown in Fig. 7b. The  
414 SPVA/RACNs-30 film presented a purple color at the beginning, then green color at  
415 90 h and finally yellow color after 135 h, while the SPVA/RACNs-60 film changed its  
416 color from initial pink to purple at 90 h and green after 150 h. As to the SPVA/RACNs-  
417 60 film, it showed a red color at first which turned to pink at 105 h and purple after 135  
418 h. These color changes indicated that the colorimetric films became more basic due to  
419 the increasing TVB-N. However, it can be observed that the SPVA/RACNs-30 film  
420 exhibited the highest color change rate, followed by the SPVA/RACNs-60 film and  
421 then the SPVA/RACNs-120 film. This was in consist with the results found in 3.2.5  
422 section in which the colorimetric films with lower content of RACNs had higher color  
423 change rates.

424 All of the colorimetric films displayed continuous color changes within the shelf  
425 life of fish (135 h), suggesting that they were capable to indicate the real-time fish  
426 freshness. Furthermore, it was well received for the colorimetric films to have rapid  
427 response to the TVB-N so that they could indicate the fish freshness in the early stages  
428 of storage. From this aspect, the SPVA/RACNs-30 film and SPVA/RACNs-60 film  
429 which presented earlier color variation were superior to the SPVA/RACNs-120 film,  
430 because the SPVA/RACNs-120 film did not show discriminative color changes until  
431 75 h. However, it was worth mentioning that the colors displayed by the  
432 SPVA/RACNs-30 film were not deep enough to be easily seen by naked eyes. These  
433 results suggested that the colorimetric film with an appropriate content of anthocyanins  
434 would be favorable to its practical application for real-time monitoring the fish

435 freshness. The colorimetric film with a high content of anthocyanins would take a long  
436 time for its color shift, while the colorimetric film containing an extremely low content  
437 of anthocyanins would present weak colors although it had rapid color changes.

438 Fig. 7

#### 439 **4. Conclusions**

440 Novel colorimetric films were successfully developed by incorporating 30, 60 and  
441 120 mg RACNs/100 g starch with SPVA through casting/solvent evaporation method.  
442 The FTIR spectra of the colorimetric films certified that RACNs were successfully  
443 immobilized into the SPVA matrix. X-ray diffraction spectra and SEM micrographs  
444 indicated that the crystallinity of PVA was reduced during the film-forming process  
445 and the compatibility between starch and PVA was improved, owing to the presence of  
446 RACNs. The incorporation of RACNs led to a decrease of water content and tensile  
447 strength, and an increase of elongation at break. The color stability test showed that the  
448 colorimetric films were stable within 14 days at 4°C and 25°C. The colorimetric film  
449 with lower content of RACNs was more sensitive to ammonia. The results of the  
450 application trial showed that the SPVA/RACNs-60 film were able to indicate the real-  
451 time fish freshness by visible color changes. All the materials used to fabricate the  
452 colorimetric films were nontoxic and biodegradable. Hence, the colorimetric films can  
453 be used as safe and eco-friendly fish freshness indicators for intelligent packaging.

454

455 **Acknowledgment**

456 The authors gratefully acknowledge the financial support provided by the national  
457 science and technology support program (2015BAD17B04, 2015BAD19B03), the  
458 national natural science foundation of China (Grant No.61301239), China postdoctoral  
459 science foundation (2013M540422, 2014T70483, 2016M590422), the national natural  
460 science foundation of China (31601543), the natural science foundation of Jiangsu  
461 province (BK20160506), science foundation for postdoctoral in Jiangsu province  
462 (1301051C), Suzhou science and technology project (SNG201503), international  
463 science and technology cooperation project of Zhenjiang (GJ2015010), research  
464 foundation for advanced talents in Jiangsu University (13JDG039) and Priority  
465 Academic Program Development of Jiangsu Higher Education Institutions (PAPD). We  
466 also would like to thank our colleagues in School of Food and Biological Engineering  
467 who provided assistance in this study.

468 **Notes**

469 The authors declare no competing financial interest.

470 **Reference**

- 471 Ajay, M., Chai, H. J., Mustafa, A. M., Gilani, A. H., & Mustafa, M. R. (2007). Mechanisms of the anti-  
472 hypertensive effect of *Hibiscus sabdariffa* L. calyces. *Journal of Ethnopharmacology*, *109*(3),  
473 388-393.
- 474 Buléon, A., Colonna, P., Planchot, V., & Ball, S. (1998). Starch granules: structure and biosynthesis.  
475 *International Journal of Biological Macromolecules*, *23*(2), 85-112.
- 476 Byrne, L., Lau, K. T., & Diamond, D. (2002). Monitoring of headspace total volatile basic nitrogen from  
477 selected fish species using reflectance spectroscopic measurements of pH sensitive films. *The*  
478 *Analyst*, *127*(10), 1338-1341.
- 479 Cai, J., Chen, Q., Wan, X., & Zhao, J. (2011). Determination of total volatile basic nitrogen (TVB-N)  
480 content and Warner–Bratzler shear force (WBSF) in pork using Fourier transform near infrared  
481 (FT-NIR) spectroscopy. *Food Chemistry*, *126*(3), 1354-1360.
- 482 Cano, A., Cháfer, M., Chiralt, A., & González-Martínez, C. (2015). Physical and Antimicrobial  
483 Properties of Starch-PVA Blend Films as Affected by the Incorporation of Natural  
484 Antimicrobial Agents. *Foods*, *5*(1), 3.
- 485 Cano, A. I., Cháfer, M., Chiralt, A., & González-Martínez, C. (2015). Physical and microstructural  
486 properties of biodegradable films based on pea starch and PVA. *Journal of Food Engineering*,  
487 *167*, 59-64.
- 488 Castañeda-Ovando, A., Pacheco-Hernández, M. d. L., Páez-Hernández, M. E., Rodríguez, J. A., &  
489 Galán-Vidal, C. A. (2009). Chemical studies of anthocyanins: A review. *Food Chemistry*,  
490 *113*(4), 859-871.
- 491 Chang, X. L., Wang, D., Chen, B. Y., Feng, Y. M., Wen, S. H., & Zhan, P. Y. (2012). Adsorption and  
492 desorption properties of macroporous resins for anthocyanins from the calyx extract of roselle  
493 (*Hibiscus sabdariffa* L.). *Journal of Agricultural and Food Chemistry*, *60*(9), 2368-2376.
- 494 Choi, I., Lee, J. Y., Lacroix, M., & Han, J. (2017). Intelligent pH indicator film composed of agar/potato  
495 starch and anthocyanin extracts from purple sweet potato. *Food Chemistry*, *218*, 122-128.
- 496 Degenhardt, A., Knapp, H., & Winterhalter, P. (2000). Separation and Purification of Anthocyanins by  
497 High-Speed Countercurrent Chromatography and Screening for Antioxidant Activity. *Journal*  
498 *of Agricultural and Food Chemistry*, *48*(2), 338-343.
- 499 Garber, K. C. A., Odendaal, A. Y., & Carlson, E. E. (2013). Plant Pigment Identification: A Classroom  
500 and Outreach Activity. *Journal of Chemical Education*, *90*(6), 755-759.
- 501 Golasz, L. B., Silva, J. D., & Silva, S. B. D. (2013). Film with anthocyanins as an indicator of chilled  
502 pork deterioration. *Ciência E Tecnologia De Alimentos*, *33*(2), 155-162.
- 503 Grajeda-Iglesias, C., Figueroa-Espinoza, M. C., Barouh, N., Barea, B., Fernandes, A., de Freitas, V., &  
504 Salas, E. (2016). Isolation and Characterization of Anthocyanins from *Hibiscus sabdariffa*  
505 Flowers. *Journal of Natural Products*, *79*(7), 1709-1718.
- 506 Guo, J., Liu, L., Lian, X., Li, L., & Wu, H. (2014). The properties of different cultivars of Jinhai sweet  
507 potato starches in China. *International Journal of Biological Macromolecules*, *67*, 1-6.
- 508 Jiang, X., Jiang, T., Gan, L., Zhang, X., Dai, H., & Zhang, X. (2012). The plasticizing mechanism and  
509 effect of calcium chloride on starch/poly(vinyl alcohol) films. *Carbohydrate Polymers*, *90*(4),  
510 1677-1684.
- 511 Kuswandi, B., Jayus, Restyana, A., Abdullah, A., Heng, L. Y., & Ahmad, M. (2012). A novel  
512 colorimetric food package label for fish spoilage based on polyaniline film. *Food Control*,

- 513 25(1), 184-189.
- 514 Lewis, C. E., Walker, J. R. L., & Lancaster, J. E. (1995). Effect of polysaccharides on the colour of  
515 anthocyanins. *Food Chemistry*, 54(3), 315-319.
- 516 Lu, D. R., Xiao, C. M., & Xu, S. J. (2009). Starch-based completely biodegradable polymer materials.  
517 *Express Polymer Letters*, 3(6), 366-375.
- 518 Ma, Q., & Wang, L. (2016). Preparation of a visual pH-sensing film based on tara gum incorporating  
519 cellulose and extracts from grape skins. *Sensors and Actuators B: Chemical*, 235, 401-407.
- 520 Olafsdóttir, G., Martinsdóttir, E., Oehlenschläger, J., Dalgaard, P., Jensen, B., Undeland, I., Mackie, I.  
521 M., Henehan, G., Nielsen, J., & Nilsen, H. (1997). Methods to evaluate fish freshness in research  
522 and industry. *Trends in Food Science & Technology*, 8(8), 258-265.
- 523 Pacquit, A., Frisby, J., Diamond, D., Lau, K., Farrell, A., Quilty, B., & Diamond, D. (2007). Development  
524 of a smart packaging for the monitoring of fish spoilage. *Food Chemistry*, 102(2), 466-470.
- 525 Pereira, V. A., de Arruda, I. N. Q., & Stefani, R. (2015). Active chitosan/PVA films with anthocyanins  
526 from Brassica oleraceae (Red Cabbage) as Time-Temperature Indicators for application in  
527 intelligent food packaging. *Food Hydrocolloids*, 43, 180-188.
- 528 Rezaei, A., Nasirpour, A., & Fathi, M. (2015). Application of Cellulosic Nanofibers in Food Science  
529 Using Electrospinning and Its Potential Risk. *Comprehensive Reviews in Food Science and  
530 Food Safety*, 14(3), 269-284.
- 531 Sin, L. T., Rahman, W. A. W. A., Rahmat, A. R., & Mokhtar, M. (2011). Determination of thermal  
532 stability and activation energy of polyvinyl alcohol-cassava starch blends. *Carbohydrate  
533 Polymers*, 83(1), 303-305.
- 534 Sinela, A., Rawat, N., Mertz, C., Achir, N., Fulcrand, H., & Dornier, M. (2017). Anthocyanins  
535 degradation during storage of Hibiscus sabdariffa extract and evolution of its degradation  
536 products. *Food Chemistry*, 214, 234-241.
- 537 Sreekumar, P. A., Al-Harhi, M. A., & De, S. K. (2012). Studies on compatibility of biodegradable  
538 starch/polyvinyl alcohol blends. *Polymer Engineering & Science*, 52(10), 2167-2172.
- 539 Sui, X., Bary, S., & Zhou, W. (2016). Changes in the color, chemical stability and antioxidant capacity  
540 of thermally treated anthocyanin aqueous solution over storage. *Food Chemistry*, 192, 516-524.
- 541 Tang, S., Zou, P., Xiong, H., & Tang, H. (2008). Effect of nano-SiO<sub>2</sub> on the performance of  
542 starch/polyvinyl alcohol blend films. *Carbohydrate Polymers*, 72(3), 521-526.
- 543 Tang, X., & Alavi, S. (2011). Recent advances in starch, polyvinyl alcohol based polymer blends,  
544 nanocomposites and their biodegradability. *Carbohydrate Polymers*, 85(1), 7-16.
- 545 Tian, S. J., Rickard, J. E., & Blanshard, J. M. V. (1991). Physicochemical properties of sweet potato  
546 starch. *Journal of the Science of Food and Agriculture*, 57(4), 459-491.
- 547 Tsai, P.-J., McIntosh, J., Pearce, P., Camden, B., & Jordan, B. R. (2002). Anthocyanin and antioxidant  
548 capacity in Roselle (Hibiscus Sabdariffa L.) extract. *Food Research International*, 35(4), 351-  
549 356.
- 550 Wang, L., Dong, Y., Men, H., Tong, J., & Zhou, J. (2013). Preparation and characterization of active  
551 films based on chitosan incorporated tea polyphenols. *Food Hydrocolloids*, 32(1), 35-41.
- 552 Wang, Z., Li, Y., Chen, L., Xin, X., & Yuan, Q. (2013). A study of controlled uptake and release of  
553 anthocyanins by oxidized starch microgels. *Journal of Agricultural and Food Chemistry*,  
554 61(24), 5880-5887.
- 555 Xiaowei, H., Xiaobo, Z., Jiewen, Z., Jiyong, S., Zhijia, L., & Tingting, S. (2015). Monitoring the  
556 biogenic amines in Chinese traditional salted pork in jelly (Yao-meat) by colorimetric sensor

- 557 array based on nine natural pigments. *International Journal of Food Science & Technology*,  
558 50(1), 203-209.
- 559 Xu, Y. X., Kim, K. M., Hanna, M. A., & Nag, D. (2005). Chitosan–starch composite film: preparation  
560 and characterization. *Industrial Crops and Products*, 21(2), 185-192.
- 561 Yoon, S.-D., Chough, S.-H., & Park, H.-R. (2006). Effects of additives with different functional groups  
562 on the physical properties of starch/PVA blend film. *Journal of Applied Polymer Science*,  
563 100(5), 3733-3740.
- 564 Zhang, X., Lu, S., & Chen, X. (2014). A visual pH sensing film using natural dyes from Bauhinia  
565 blakeana Dunn. *Sensors and Actuators B: Chemical*, 198, 268-273.
- 566 Zhang, X., Sun, G., Xiao, X., Liu, Y., & Zheng, X. (2016). Application of microbial TTIs as smart label  
567 for food quality: Response mechanism, application and research trends. *Trends in Food Science  
568 & Technology*, 51, 12-23.
- 569

**Figure captions**

**Fig. 1.** (a) Color and (b) UV-vis spectra of RACNs solution (0.12 mg/mL) at pH 2-12.

**Fig. 2.** FTIR spectra of (a) starch, (b) PVA, (c) RACNs, (d) SPVA film, (e) SPVA/RACNs-30 film, (f) SPVA/RACNs-60 film and (g) SPVA/RACNs-120 film.

**Fig. 3.** XRD spectra of starch, PVA, SPVA film, SPVA/RACNs-30 film, SPVA/RACNs-60 film and SPVA/RACNs-120 film.

**Fig. 4.** SEM micrographs of the cross sections of (a) SPVA film, (b) SPVA/RACNs-30 film, (c) SPVA/RACNs-60 film, and (d) SPVA/RACNs-120 film.

**Fig. 5.** The relative color change ( $S$ ) of the colorimetric films stored at 4°C and 25°C for 14 d.

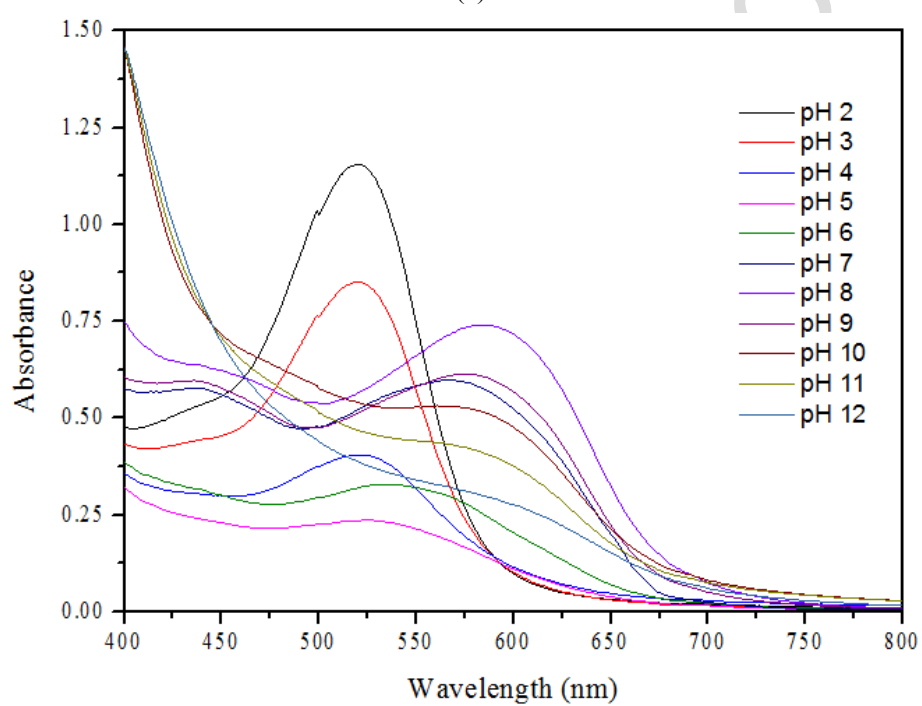
**Fig. 6.** UV-vis spectra of (a) SPVA/RACNs-30 film, (b) SPVA/RACNs-60 film and (c) SPVA/RACNs-120 film when exposed to ammonia generated from a 8 mM ammonia solution at 25°C for 24 min, and (d) the change of the absorbance ratio at 640 nm versus 540 nm ( $A_{640}/A_{540}$ ).

**Fig. 7.** (a) The change of TVB-N level of stored silver carp within 165 h at 4°C and (b) the corresponding color changes of the colorimetric films.

Fig. 1



(a)



(b)

Fig. 2

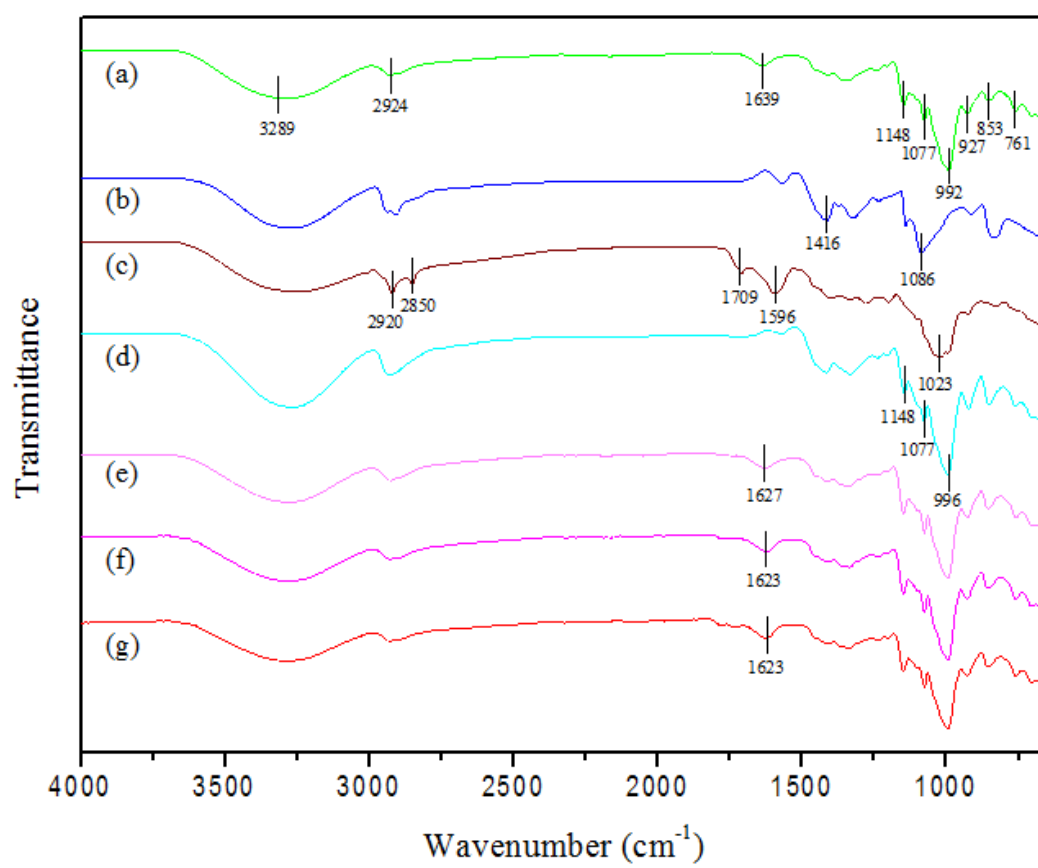


Fig. 3 revision FOOHYD 3804

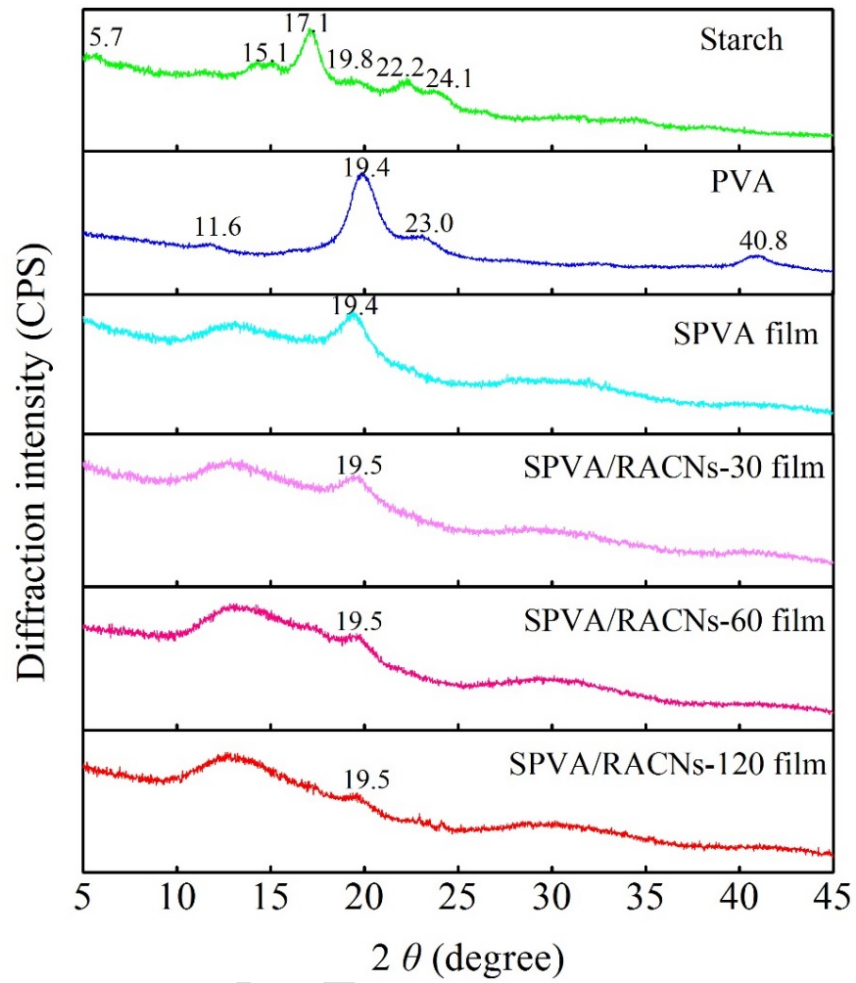


Fig. 4

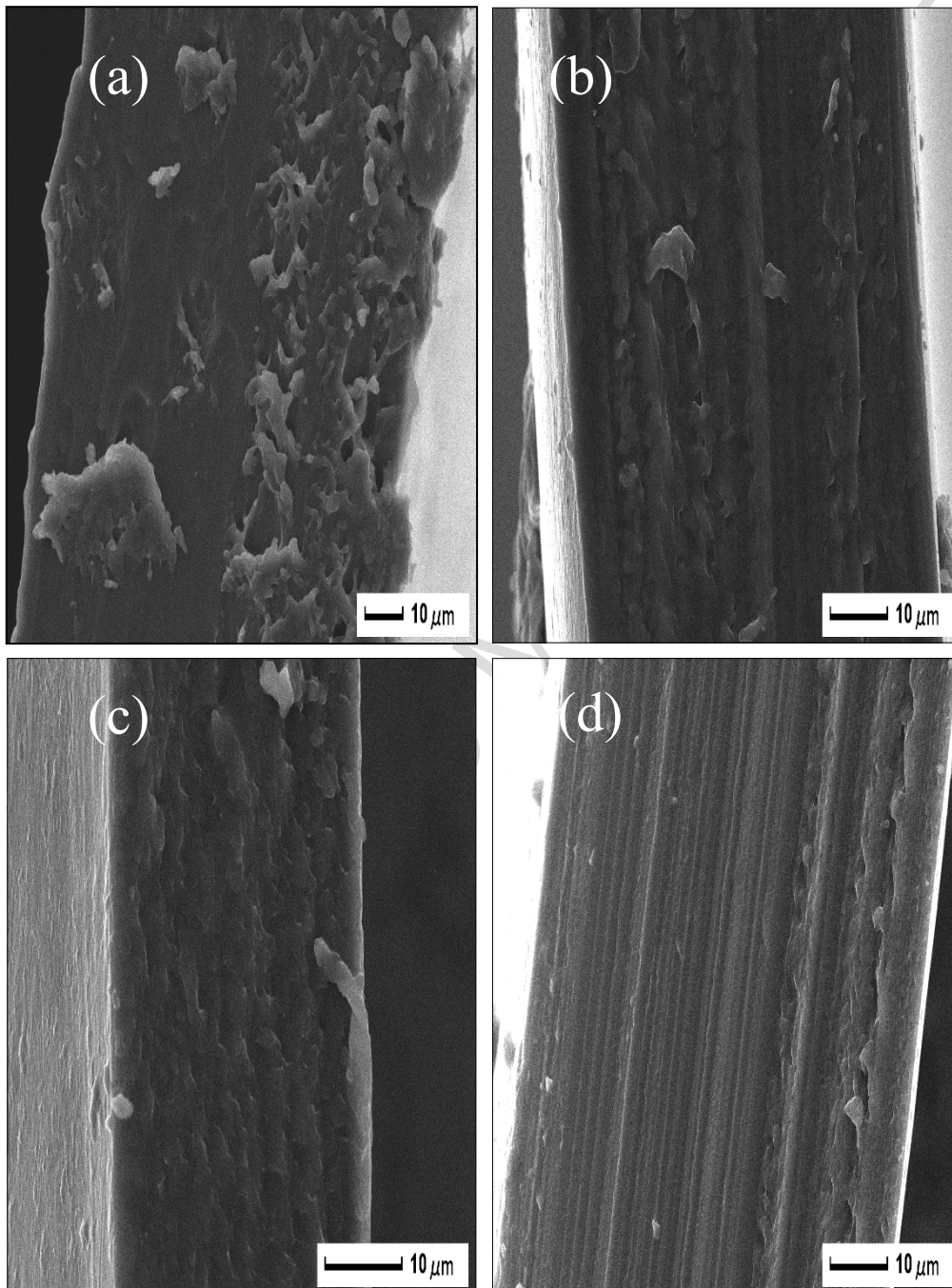


Fig. 5

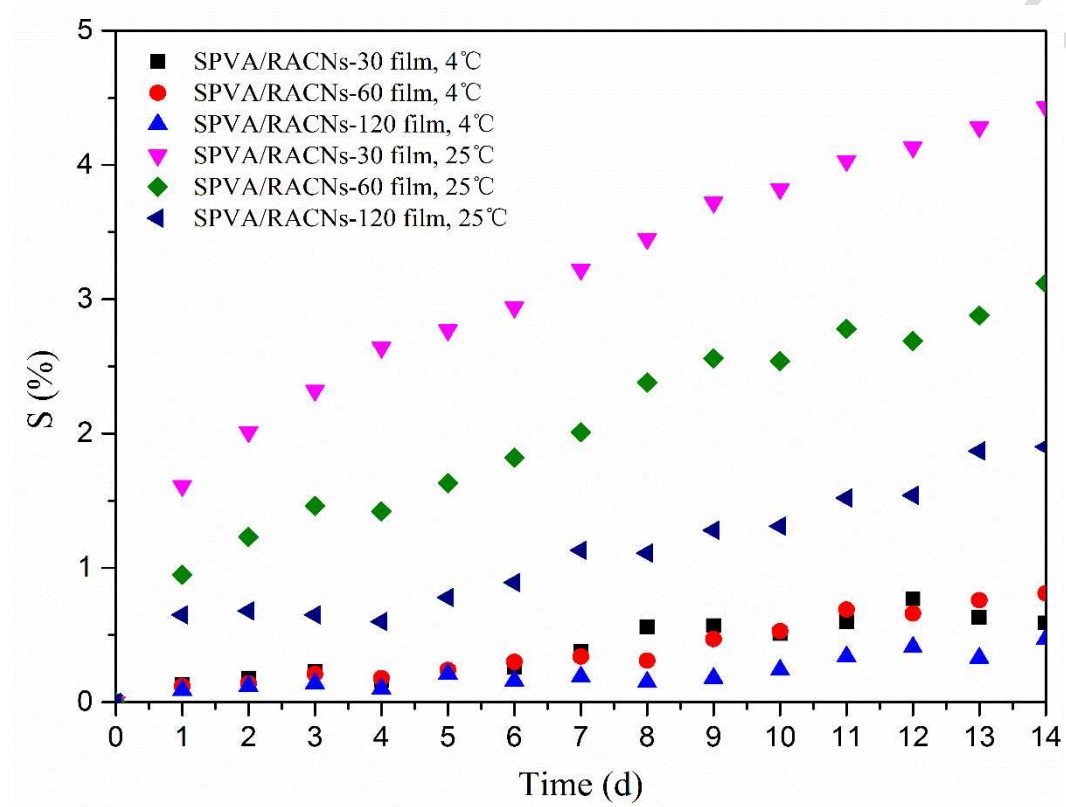


Fig. 6

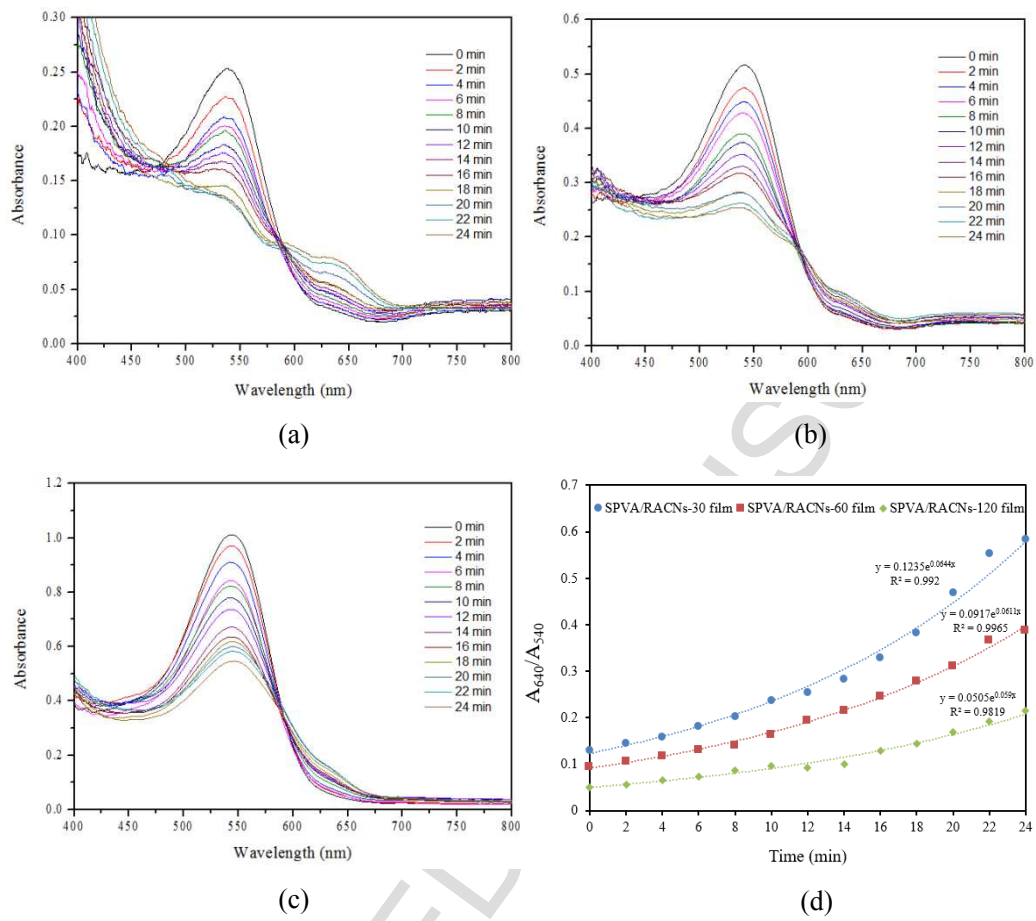
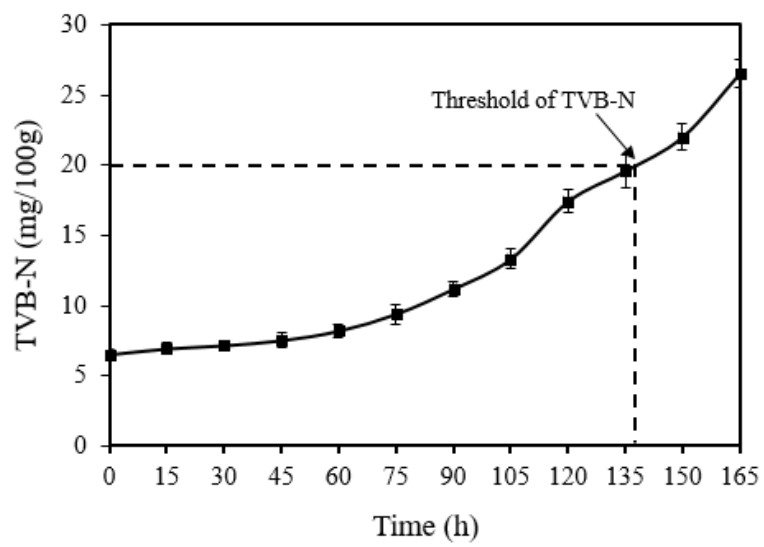
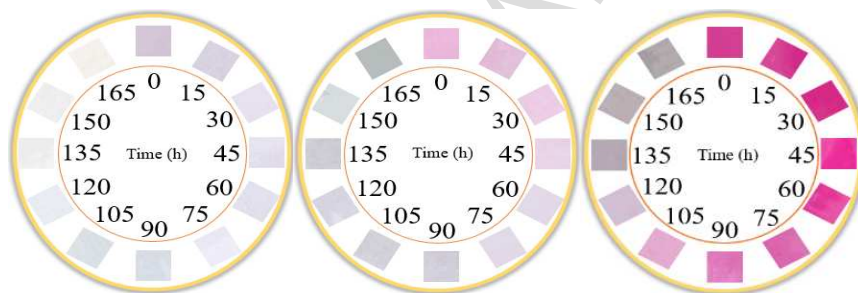


Fig. 7



(a)



SPVA/RACNs-30 film    SPVA/RACNs-60 film    SPVA/RACNs-120 film

(b)

**Table 1**

Thickness, water content, tensile strength and elongation at break of the SPVA film and the colorimetric films.

Films	Thickness ( $\mu\text{m}$ )	Water content (%)	Tensile strength (MPa)	Elongation at break (%)
SPVA	$88.06 \pm 3.10^b$	$25.50 \pm 0.98^a$	$48.97 \pm 2.36^a$	$44.15 \pm 2.42^d$
SPVA/RACNs-30	$88.40 \pm 3.21^b$	$25.21 \pm 1.47^a$	$48.21 \pm 2.60^a$	$49.12 \pm 2.09^c$
SPVA/RACNs-60	$89.25 \pm 2.57^b$	$22.04 \pm 1.33^b$	$45.17 \pm 1.78^b$	$60.24 \pm 3.18^b$
SPVA/RACNs-120	$93.89 \pm 3.13^a$	$18.50 \pm 0.98^c$	$41.85 \pm 2.03^c$	$88.28 \pm 3.51^a$

Data were presented as mean  $\pm$  standard deviation of three samples.

Data in the same column with different letter were significantly different ( $p < 0.05$ ).